Practical Kicking Motion Generation Method for NAO

Chaojun Wang, Wenchuan Jia*, Yi Sun, Shugen Ma
School of Mechatronic Engineering and Automation
Shanghai Key Laboratory of Intelligent Manufacturing and Robotics
Shanghai University
Shanghai, China
*Corresponding author: lovvchris@shu.edu.cn

Abstract – **This paper proposed a practical method of generating the omnidirectional kicking motion for NAO robot which has ability to kick in different directions. The method consists of two systems, that are the vision and neural network based distance measurement system (DMS), and the kicking motion generating system (KMGS). The DMS obtains the coordinate of the football and the target point (TP) in the specified coordinate system according to their pixel value in single image. Then the KMGS plans the trajectory of swinging leg and generates kicking motion online based on the coordinate of ball and TP. The experimental results of NAO robot show that the proposed systems perform well and complete the kicking mission effectively.**

Index Terms – NAO robot, Kicking motion, Neural network.

I. INTRODUCTION

RoboCup is the most well-known robot football game in the world. With the continuous development, its standard platform, NAO robot, has also been widely used. In a robot football game, it is important to obtain the coordinate of the football and the target point (TP) accurately, and generate the kicking motion rapidly.

In RoboCup, the standard ball with red color is used to instead the real football and the coordinate of ball and TP is generally obtained by the visual system of NAO robot. The dominant vision based distance measurement methods always use a binocular stereo system [1][2]. In addition, there is also a monocular vision system. For example, Gao et al. take two single images by a zoom camera to complete the 3D reconstruction model of zooming images [3]. However, NAO robot still uses a traditional monocular vision system with fixed focal length of its camera. So the above methods are not suitable for NAO robot. Assuming that the height of the camera and the ball and TP are constant, the tilt angle of camera is fixed during the measurement process. Then, the geometrical distance measurement methods can be adopted to establish the transformation between image plane coordinate and world coordinate [4][5]. Nevertheless, the effect of the geometrical methods is affected by lens distortion [4], and the transformation is highly nonlinear [6].

For the different coordinate of ball and TP, it cannot achieve accurate and fast kicking motion by adopting the animation method which uses series of fixed keyframes that are recorded in advance. So an online method for generating the kicking motion dynamically is necessary. Je Youn Choi et al. deal with the trajectory planning of a ball driven by a kicking robot [7], they use an algorithm to control the arrival time and the arrival distance of the ball, and achieve the goal of passing and shooting. Rafael Cisneros et al. propose an algorithm that enables a humanoid robot to kick a ball which can fly to a desired 3D goal position [8][9]. These algorithms can generate kicking motion according to different conditions. However, they mainly focus on the motion itself or cannot be performed directly by the NAO robot for realizing curving ball and volley pass. Bo Fan et al. control the NAO robot to kick a ball into a goal just in RoboCup3D simulation game [10][11], but do not perform on a real NAO robot, because the game environment is quite different from the real situation.

In this paper, the distance measurement system (DMS) and the kicking motion generating system (KMGS) has been introduced to complete the omnidirectional kick of NAO robot. Section II explains the DMS which employs a multilayer neural network (MNN) to obtain the coordinate of ball and TP relative to NAO robot. Section III explains the KMGS which employs two polynomials to fit the trajectory of swinging leg and generate kicking motion online based on the output of the DMS. Section IV shows the overall process of the omnidirectional kick and tests the effectiveness of the DMS and KMGS. The final section concludes this paper and puts forward the future works.

II. DISTANCE MEASUREMENT SYSTEM (DMS)

The method which is used to build the model of the DMS, i.e., MNN and obtain the coordinate of ball and TP relative to NAO robot, is described in this section. This model will provide input value for the KMGS.

A. Coordinate Systems

Before all the discussions, we specify each coordinate systems as in Fig. 1. The world coordinate system, $\{W\}$, is located at the kickoff point of football field. The plane formed by x-y axis is parallel to horizontal plane, and the z axis is straight up. The ball coordinate system, $\{B\}$, is located in the center of the ball. The x axis changes according to the kicking direction $\mathbf{K}$, and the z axis is straight up. The robot coordinate system, $\{R\}$, is located at the midpoint of two support legs. The x axis is oriented the same as NAO robot, and the z axis is straight up. And the image coordinate system, $\{I\}$, which is a two dimensional coordinate system, is located at the midpoint of image's bottom edge. The x axis is straight up and the y axis is horizontal to the left.
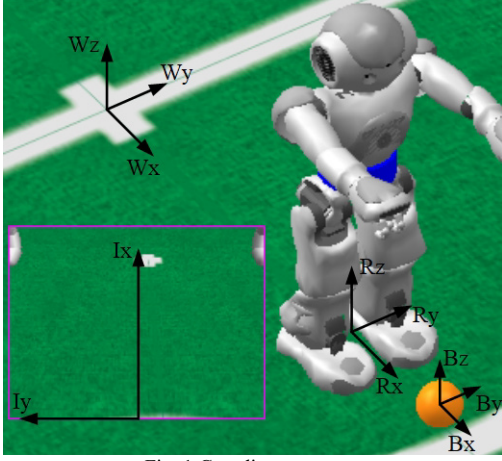
Fig. 1 Coordinate systems

B. Multilayer Neural Networks (MNN)

Measuring the coordinate of ball and TP in football field has many constraints. When the camera of NAO robot takes an image, its height relative to the ground is constant, and tilt angle relative to the horizontal plane is fixed. Therefore, for the same tilt angle of camera, there is a nonlinear relationship between the value of x, y coordinate in {I} and in {R}. It is known that a neural network is suitable for the (especially nonlinear) function approximation via various learning algorithms [12]. In this section, the MNN is used to establish the transformation between {I} and {R}, and calculate the coordinate of ball and TP in {R}, i.e., $p_{Bo} = [p_{Box}, p_{Boy}, r_B]^T$ and $p_T = [p_{Tx}, p_{Ty}, r_B]^T$, by their pixel value in {I}. Where r_B is the radius of ball.

The first step is to get training data and test data. When the NAO robot stands on the ground, the view for yaw angle $\alpha = 0°$ and pitch angle $\beta = 25°$ is shown in Fig. 2. The quadrilateral region of Fig. 2(a) corresponds to Fig. 2(b), i.e., the visible range of NAO robot in above situations. Manually measuring the sets of coordinate of balls in {R}, i.e., (x_R, x_R), as shown in Fig. 2(a). Then taking images to get the pixel value of balls in {I}, i.e., (x_I, x_I), as shown in Fig. 2(b). Each sets of (x_R, x_R) and (x_I, x_I) are used as the input and label of MNN respectively. We select 425 sets of training data to train our MNN and 20 sets of test data to verify it.

In the second step, a five-layer neural network including an input layer, three hidden layers, and an output layer is built. The number of neurons in the input layer and hidden layer is 2, 4, 8 and 4 respectively, whose forward propagation model is as (1).

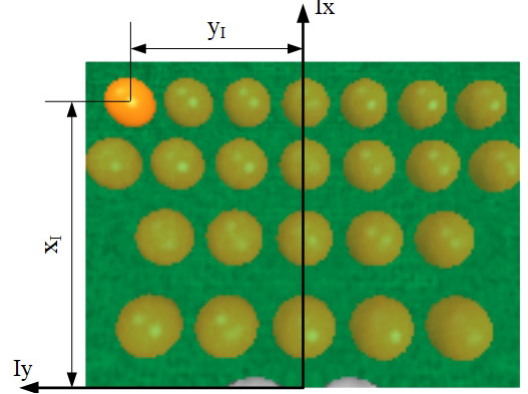$$y_l = f(u_l) = f(W_l y_{l-1} + b_l) \quad (1)$$

The number of neurons in the output layer is 2, whose forward propagation model is as (2).

$$y_l = u_l = W_l y_{l-1} + b_l \quad (2)$$

Where $f(\cdot)$ is activation function which uses ReLU unit. W_l and b_l are weighting and basing matrices in the lth layer. y_l is the output of the lth layer.
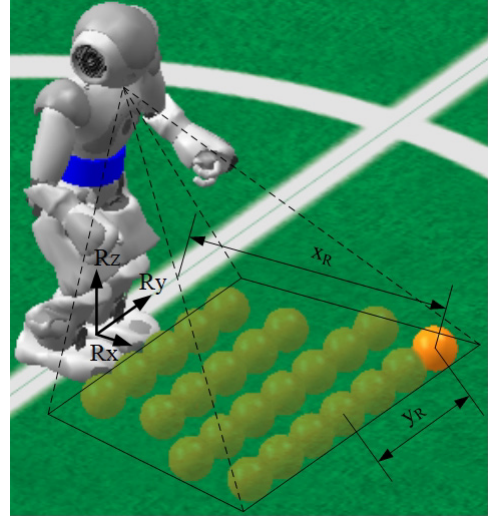
(a) Positional relationship between NAO robot and ball

(b) Image taken by the camera of NAO robot
Fig. 2 View for $\alpha = 0°$ and $\beta = 25°$

The mean square error is used as loss function, as (3).

$$MSE = \frac{1}{n} \sum_{i=1}^{n} (y_i - y_i^p)^2 \quad (3)$$

The weight and bias are optimized by gradient descent method, as (4).

$$x_l := x_l - \eta \frac{\partial E}{\partial x_l} \quad (4)$$

The above MNN is trained by the training data and test data obtained in the first step. This process obtains the trained MNN which has optimal weighting and biasing matrices. When NAO robot takes an image and gets the pixel value of ball in {I}, the trained MNN can use the pixel value to estimate the coordinate of ball in {R}, even if the pixel value is not one of the inputs of training data and test data. The process is shown in Fig. 3. The coordinate of TP is estimated like the ball. If the coordinate of ball is outside of the reachability grid of NAO robot's leg [13], the NAO robot is commanded to approach the ball according to p_{Bo} firstly, and then estimates the coordinate of the ball again which is located at the reachability grid. Finally, taking the estimated p_{Bo} and p_T as input to the KMGS.
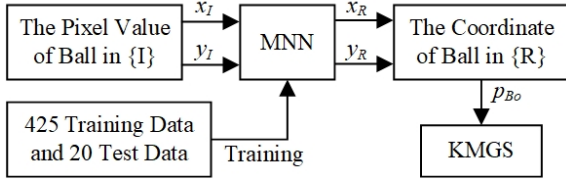
164

Fig. 3 Estimating the coordinate of ball in {R} by the pixel value in {I}

III. KICKING MOTION GENERATING SYSTEM (KMGS)

Due to the walking error, there is uncertainty between the relative position of NAO robot and ball. If a fixed kicking motion is used by means of the keyframe method, the NAO robot has to be fine-tuned to the specified position to satisfy the uncertain positional relationships. This method is very time consuming and needs high precision short distance movement for NAO robot. It has poor practicality and effect.

Based on the coordinate of ball and TP which obtained by above DMS, this section dynamically plans the contact point on the ball, the contact point on the foot and the kicking motion of swinging leg by the KMGS. This method does not require fine-tuning the position of NAO robot, but instead generating a kicking motion online to complete the omnidirectional kick.

A. Analysis of the Contact Point on the Ball

In order to make the ball move as fast as possible, this paper specifies that the NAO robot plays with the fastest kicking speed and the horizontal component of kicking direction **K** (hereinafter referred to as kicking direction **K**) points to the center of ball. Fig. 4 is the planform of the ball and its coordinate systems. Where the x axis changes according to the kicking direction **K**. θ is the angle between kicking direction **K** and x axis of {R}. $^{B}p_{Bc}$ is the coordinate of contact point on the ball in {B}, and its value is $^{B}p_{Bc} = [-r_{B}, 0, 0]^{T}$.

The coordinate of ball and TP, p_{Bo} and p_{T}, can be obtained according to the DMS to select a suitable swinging leg and a TP on both sides of goal. The criterion is as follows: When $p_{Boy} < 0$, the right leg is selected as swinging leg, and the left side of goal is selected as the TP, i.e., using the right leg to kick the ball to the TP which on the left side of goal. When $p_{Boy} \geq 0$, it is inverted. Then, the angle between kicking direction **K** and x axis of {R}, and the rotation matrix of {B} with respect to {R}, i.e., θ and R_{B}, can be calculated as (5) and (6).

$$\theta = \tan^{-1} \frac{p_{Ty} - p_{Boy}}{p_{Tx} - p_{Box}} \tag{5}$$

$$R_{B} = \begin{bmatrix} \cos\theta & -\sin\theta & 0 \\ \sin\theta & \cos\theta & 0 \\ 0 & 0 & 1 \end{bmatrix} \tag{6}$$

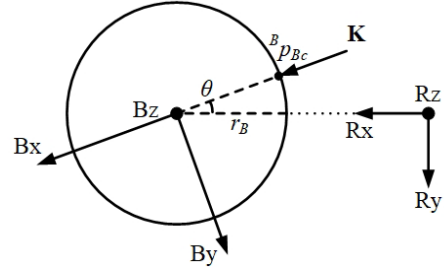The coordinate of contact point on the ball in {R}, p_{Bc}, can be calculated as (7).
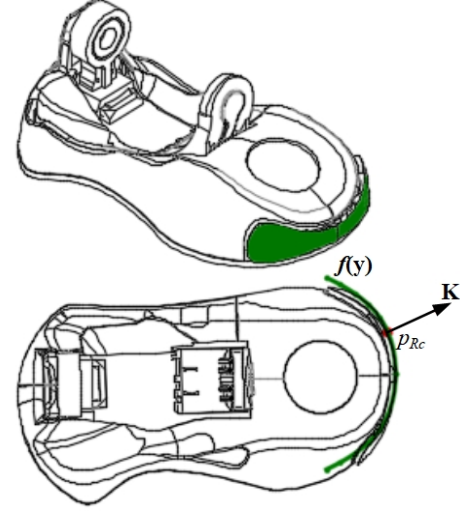

Fig. 4 Planform of the ball and its coordinate systems

Fig. 5 Contact point (red point) and fitted contour (green curve)

$$p_{Bc} = p_{Bo} + R_{B}{}^{B}p_{Bc} = \begin{bmatrix} p_{Box} - r_{B}\cos\theta \\ p_{Boy} - r_{B}\sin\theta \\ p_{Boz} \end{bmatrix} \tag{7}$$

B. Analysis of the Contact Point on the Foot

The kicking process of NAO robot is complicated, and not all of the motion trajectories need to be generated online. Then the kicking motion is divided to four phases. In the incline phase, NAO robot shifts the center of gravity to the support leg. In the traction phase, robot retracts the swinging leg. In the kicking phase, robot executes the kicking motion. In the wrap-up phase, robot returns to standing position and ends the kicking process.

In these four phases, only the kicking phase needs to be generated online. To generate the kicking motion, the coordinate of contact point on the foot in {R}, p_{Rc}, has to be calculated. It has to be estimated that which part of the foot contact the ball. So we manually measure the shape of the front contour of the foot in {R} and adopt least square fits [14] to fit the measured data. The fitted contour function of foot is shown as (8) and the fitting result is shown in Fig. 5, which shows that the inner side of foot has a better fitting effect than the outer side. Since the kicking motion always uses the inner side of foot to kick the ball, equation (8) is adopted.

$$f(y) = -7523.85y^{4} - 1504.76y^{3} - 122.64y^{2} - 4.74y + 0.03 \tag{8}$$

Because the contour is approximately circular, the kick state is approximately to a collision between two spheres. So

the tangent at the contact point needs to be orthogonal to the kicking direction **K**. Thus, the contact point, p_{Rc}, can be calculated by associating the contour function $f(y)$ and its derivative, $f'(y) = \tan\theta$, as shown in Fig. 5.

C. Online Generation of the Kicking Motion of Swinging Leg

The motion of swinging leg needs to be generated online to kick the ball. Therefore, a kicking trajectory followed by the contact point on the foot needs to be planned. Polynomials method is a solution in motion generation because it can obtain smooth curves. Then, the two cubic polynomials, as (9) and (10), which fit two kicking trajectories are used. The first is the initial position of contact point to the position when the ball is in contact with foot, i.e., $p_{Rc,0}$ - $p_{Rc,k}$. The second is the position $p_{Rc,k}$ to the final position of contact point, i.e., $p_{Rc,k}$ - $p_{Rc,f}$. Both the curves are in the vertical plane where the kicking direction **K** is located.

$$q_1(t) = a_{10} + a_{11}t + a_{12}t^2 + a_{13}t^3 \qquad (9)$$

$$q_2(t) = a_{20} + a_{21}t + a_{22}t^2 + a_{23}t^3 \qquad (10)$$

where $a_{10},...,a_{23} \in R^3$.

In order to generate desired kicking trajectory online, specific constraints including position, speed and acceleration demands need to be put upon above two polynomials. The constraints are shown as (11) - (17).

$$q_1(0) = a_{10} = p_{Rc,0} \qquad (11)$$

$$q_1'(0) = a_{11} = 0 \qquad (12)$$

$$q_2(t_f) = a_{20} + a_{21}t_f + a_{22}t_f^2 + a_{23}t_f^3 = p_{Rc,f} \qquad (13)$$

$$q_2'(t_f) = a_{21} + 2a_{22}t_f + 3a_{23}t_f^2 = 0 \qquad (14)$$

$$q_1(t_k) = q_2(0) = a_{10} + a_{12}t_k^2 + a_{13}t_k^3 = a_{20} = p_{Rc,k} \quad (15)$$

$$q_1'(t_k) = q_2'(0) = 2a_{12}t_k + 3a_{13}t_k^2 = a_{21} \qquad (16)$$

$$q_1''(t_k) = q_2''(0) = 2a_{12} + 6a_{13}t_k = 2a_{22} \qquad (17)$$

Then, a system of linear equation with eight unknown parameters which takes the coefficients of above two polynomials as variables can be calculated. The equation is shown as (18).

$$\begin{aligned} A[a_{10} \ a_{11} \ a_{12} \ a_{13} \ a_{20} \ a_{21} \ a_{22} \ a_{23}]^T \\ = [q_1(0) \ 0 \ q_2(t_f) \ 0 \ 0 \ 0 \ 0 \ q_1(t_k)]^T \end{aligned} \qquad (18)$$

Finally, the coordinate of $p_{Rc,0}$, $p_{Rc,k}$, and $p_{Rc,f}$ need to be determined. In these three nodes, the contact point on the foot coincides with the contact point on the ball when the foot is in contact with the ball, i.e., $p_{Rc,k} = p_{Bc}$. $p_{Rc,0}$ and $p_{Rc,f}$ have little effect on the outcome of kick. The only demand is that they are in the vertical plane where the kicking direction **K** is located.

The coefficient of above two polynomials is calculated by solving (18), i.e., the kicking trajectory of the contact point on the foot is obtained. And then the kicking motion can be executed by inverse kinematics of NAO robot.
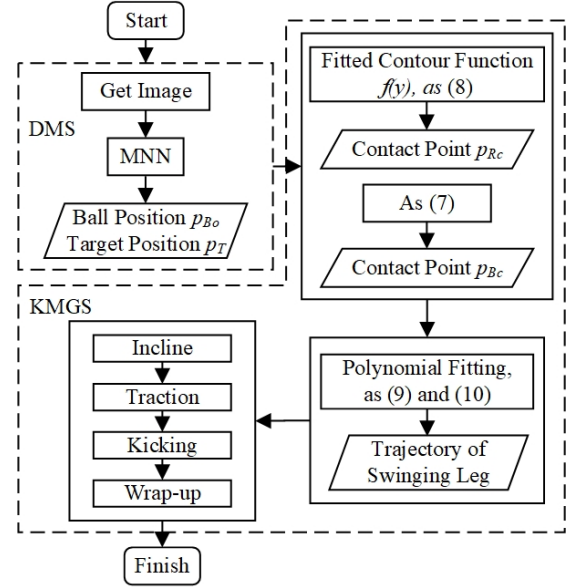

Fig. 6 Flow chart of the omnidirectional kick

IV. EXPERIMENTS AND RESULTS

This section combines the DMS and KMGS to accomplish the omnidirectional kick of NAO robot. Fig. 6 shows the kicking process. The effectiveness of above two systems are tested on a real NAO robot by using the right leg to kick the ball to the TP which on the left side of goal. Table I shows the environment of experiments.

TABLE I
ENVIRONMENT PARAMETERS

Parameter	Value
Radius of ball (r_B)	0.0325 [m]
Height of camera (h)	0.4594 [m]
Colour of ball	red
Colour of goal	white
Colour of ground	green

A. Experiment of the DMS

After 100,000 iterations, the partial curve of training loss is shown in Fig. 7. Although the training process takes a long time, it only needs to be run once. We save the trained MNN which has optimal weighting and biasing matrices and upload it to the NAO robot. When NAO robot needs to measure the distance of ball, it takes the pixel value of ball in {I} as an input to the trained MNN. And then, the output of trained MNN is the estimated coordinate of ball in {R}, p_{Bo}. It only takes a little time.

An experiment which measures the different coordinate of ball is made to evaluate the effective of the MNN. We set up twenty trials. The results are shown in Fig. 8. The blue points represent actual values and the red points represent theoretical values. In these trials, the average error is [0.00339, 0.00566], and the standard deviation is [0.02786, 0.02540]. The test data whose error, i.e., the difference between actual and theoretical value, in the range of standard deviation is more than 68%. It indicates that the DMS has good effectiveness.
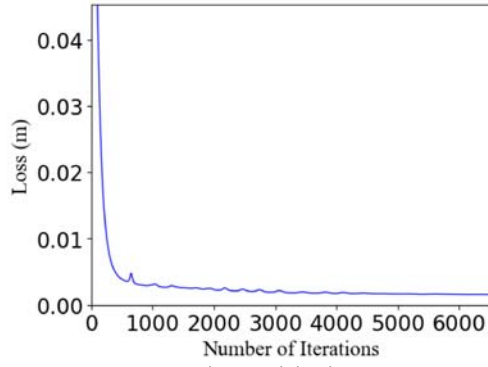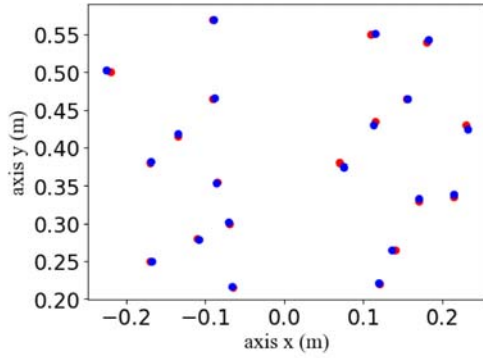
166

Fig. 7 Training loss

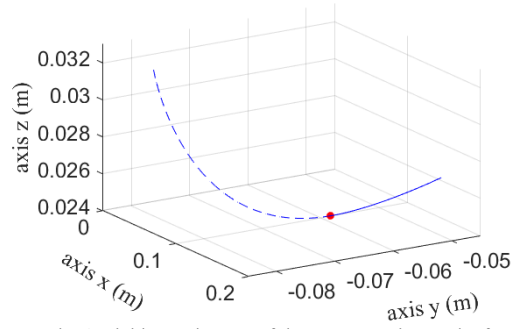Fig. 8 Twenty trials of measuring the different coordinate of ball

Fig. 9 Kicking trajectory of the contact point on the foot

Fig. 10 Kicking motion of NAO robot

Fig. 11 Twenty trials of rolling direction θ

B. Experiment of the KMGS

The coordinate of ball and TP, p_{Bo} and p_T, can be calculated according to the DMS. In order to test the kicking motion, this section first uses fixed p_{Bo} and p_T, which are listed in Table II.

TABLE II
VALUE OF p_{Bo} AND p_T

Parameter	Value
Ball (p_{Bo})	$[0.15, -0.05, r_B]^T$ [m]
TP (p_T)	$[2, 0.6, r_B]^T$ [m]

Then, p_{Bc} and p_{Rc} of the contact point can be calculated, and the kicking motion in Cartesian coordinate system can be obtained. Fig. 9 shows the kicking trajectory of the contact point on the foot. The dotted curve represents the trajectory between $p_{Rc,0}$ and $p_{Rc,k}$. The solid curve represents the trajectory between $p_{Rc,k}$ and $p_{Rc,f}$. And the red point represents the contact point. Fig. 10 shows the kicking motion of NAO robot, and the three postures represent the kicking motion in different time.

An experiment which kicks the ball to a given target is made to evaluate the effective of the kicking motion. We set up twenty trials. Since it is not easy to predicate whether the ball reaches the given target, we record the rolling direction θ of the ball to evaluate the effectiveness of kick. The results are shown in Fig. 11. The 14th test data is quite diffe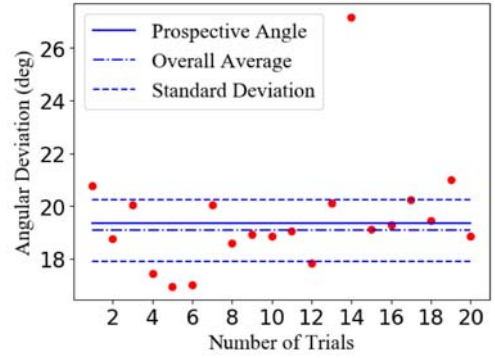rent from other test data, so this set of data is not used. In the rest of nineteen trials, the overall average is 19.07° that is marked in dash dot line. The theoretical angle is 19.36° that is marked in solid line. And the standard deviation is 1.16°. The test data which in the range of standard deviation (17.91° - 20.52°) are more than 68%. It indicates that the KMGS has good effectiveness.

Then, two experiments are made for different cases of the coordinate of p_{Bo} and p_T. In the first experiment, let $p_{Bo} = [0.15, -0.05, r_B]^T$ and $p_{Tx} = 1.7$, and use seven different p_{Ty}. In the second experiment, let $p_T = [1.7, 0.55, r_B]^T$, and use nine different p_{Bo}. For each kicking motion we execute twenty kicks and record the successful times whose rolling direction bias is located in $\{-1.5°, 1.5°\}$ compared to the theoretical value.
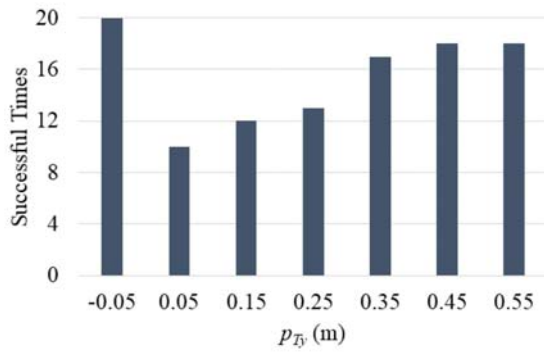
167

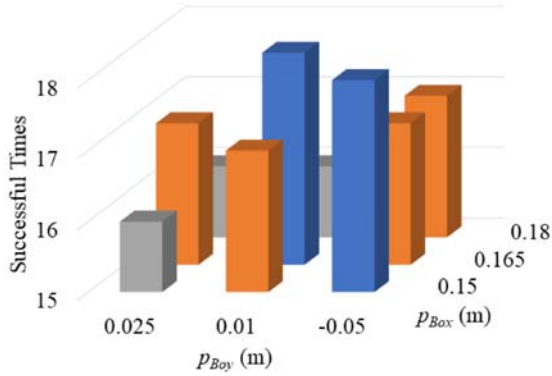Fig. 12 Kicking results with different p_{Ty}

Fig. 13 Kicking results with different p_{Bo}

Fig. 12 shows the results of the first experiment. It can be observed that the kicking motion performs well when the rolling direction θ is 0° or large (approximately more than 15°, as (5)), and not very well when θ is small except 0°. It may be because the contour of foot of NAO is not so regular. Fig. 13 shows the results of the second experiment. It can be observed that the kicking motion performs well for the different coordinate of ball.

V. CONCLUSION AND FUTURE WORK

In this paper, the omnidirectional kicking motion for NAO robot which consists of the DMS and KMGS is proposed. The DMS takes the pixel value of ball and TP in {I} as input, and then estimates their coordinate in {R} by MNN. The KMGS dynamically plans the contact point on the ball, the contact point on the foot and the kicking motion of swinging leg, and then generates and performs the kicking motion in real time.

Experiments results show that the system has good effectiveness in a free-kick situation. The future work would focus on other situations. For example, adding a defensive robot in front of the goal, or considering the situation include dribbling or stopping.

REFERENCES

[1] H. M. Long, H. Y. Guo, F. Liang, and G. H. Liu, "Distance Measurement Algorithm Based on Binocular Stereo Vision, "*Applied Mechanics and Materials*, vol. 635-637, pp. 948-952, 2014.

[2] Z. Meng, X. Kong, L. Meng and H. Tomiyama, "Distance Measurement and Camera Calibration based on Binocular Vision Technology," *International Conference on Advanced Mechatronic Systems*, Zhengzhou, 2018, pp. 342-347.

[3] H. W. Gao, J. G. Liu, Y. Yu, and Y. M. Li, "Distance measurement of zooming image for a mobile robot," *International Journal of Control, Automation and Systems*, vol. 11, no. 4, pp. 782-789, August 2013.

[4] C. J. Hsu, M. Lu, and Y. Lu, "Distance and Angle Measurement of Objects on an Oblique Plane Based on Pixel Number Variation of CCD Images," *IEEE Transactions on Instrumentation and Measurement*, vol. 60, no. 5, pp. 1779-1794, May 2011.

[5] S. W. Chen, X. Y. Fang, J. B. Shen, L. B. Wang, and L. Shao, "Single-Image Distance Measurement by a Smart Mobile Device," *IEEE Transactions on Cybernetics*, vol. 47, no. 12, pp. 4451-4462, December 2017.

[6] E. Menegatti, A. Pretto, A. Scarpa, and E. Pagello, "Omnidirectional vision scan matching for robot localization in dynamic environments," *IEEE Transactions on Robotics*, vol. 22, no. 3, pp. 523-535, June 2006.

[7] J. Y. Choi, B. R. So, B. J. Yi, W. Kim, and I. H. Suh, "Impact Based Trajectory Planning of a Soccer Ball in a Kicking Robot," *IEEE International Conference on Robotics and Automation*, Barcelona, Spain, 2005, pp. 2834-2840.

[8] R. Cisneros, K. Yokoi, and E. Yoshida, "Impulsive pedipulation of a spherical object for reaching a 3D goal position," *IEEE-RAS International Conference on Humanoid Robots*, pp. 154-160, 2013.

[9] R. Cisneros, K. Yokoi, and E. Yoshida, "Impulsive Pedipulation of a Spherical Object with 3D Goal Position by a Humanoid Robot: A 3D Targeted Kicking Motion Generator," *International Journal of Humanoid Robotics*, vol. 13, no. 2, pp. 1650003 (43), June 2016.

[10] B. Fan, and Z. Liang, "Omnidirectional kick in RoboCup3D simulation," *IEEE International Conference on Mechatronics and Automation*, Tianjin, 2014, pp. 1058-1062.

[11] X. J. Li, Z. W. Liang, and H. H. Feng, "Kicking motion planning of Nao robots based on CMA-ES," *Chinese Control and Decision Conference*, Qingdao, 2015, pp. 6158-6161.

[12] F. J. Li, "Function Approximation by Neural Networks," *Lecture Notes in Computer Science*, vol. 5263 LNCS, no. PART 1, pp. 384-390, 2008.

[13] Y. Xu, and H. Mellmann, "Adaptive Motion Control: Dynamic Kick for a Humanoid Robot," *Lecture Notes in Computer Science*, vol. 6359 LNAI, pp. 392-399, 2010.

[14] J. Zunic, and J. Koplowitz, "Representation of digital parabolas by least-square fit." *The International Society for Optical Engineering*, vol. 2356, pp. 71-78, 1995.